JOURNAL OF APPLIED ELECTROCHEMISTRY 15 (1985) 581–590

*Bubble characteristics and aerosol formation in electrowinning cells**

A. PAPACHRISTODOULOU, F. R. FOULKES, J. W. SMITH

Department of Chemical Engineering and Applied Chemistry, University of Toronto, Toronto, Ontario, M5S 1A4, Canada

Received 12 November 1984

The nature of the aerosol emitted from a scale model zinc electrowinning system, operated under industrial conditions, has been established as a function of bubble formation rate, electrode surface characteristics, coalescence of bubbles, and control strategies. The emitted aerosol was collected and characterized using an Andersen Ambient Impactor. The effect of the relative humidity of the ambient air on the composition and density of the aerosol droplets was determined, permitting comparison of emissions on a standard basis. The size distribution of the aerosol was found to be of a bimodal nature indicating the presence of both film and jet droplets of geometric mean size 2 and 30 μm respectively. The amount and distribution of the aerosol were found to depend on the bubble size distribution in the cell which in turn depends on the anode surface, the amount and nature of the MnO_2 scale and surface active substances in the electrolyte. The gross emission rate was about 2–3 mg m^{-2} s^{-1} without any control. A new method of control of the acidic emissions is proposed based on observations made and results obtained from the study of the aerosol characteristics. Providing means of enhancing bubble coalescence below the electrolyte surface results in fewer and larger bubbles which yield less aerosol. The method has been evaluated in both zinc and copper electrowinning and leads to reduction of aerosol emission by over 90%.

1. Introduction

During the electrowinning of zinc and copper in electrolytic cells, gases are evolved (oxygen at the anode and depending on current efficiency, hydrogen at the cathode) which results in the formation of bubbles. These bubbles move upwards between the electrodes and burst on the electrolyte surface, generating a large number of droplets in a variety of sizes, which form the acidic aerosol found above the cells. They also induce circulation and mixing of the electrolyte. Sulphuric acid concentrations in the air above the cell have been observed at more than 10–20 mg m^{-3} well above the threshold limit value (TLV) of 1 mg m^{-3} and emission rates of about 2–3 mg m^{-2} s^{-1} were observed in this work.

Control strategies which have been practised so far involve the use of frothing agents in the electrolyte, floating layers of balls, pellets or cylinders and hoods around the tanks in combination with good ventilation of the tankrooms. These have their obvious limitations for the operator. The purpose of the present study was to characterize the acidic aerosol emitted from zinc electrowinning cells and to clarify its mechanism of production in order to facilitate the evaluation of the existing control methods and the development of new ones. The ideal control system should be effective, non-interfering, convenient and inexpensive.

It is known that larger bubbles bursting on the electrolyte surface result in reduced aerosol emissions for a given production rate, since fewer bubbles are bursting and fewer droplets per bubble are generated. Hence, means of enhancing

* Paper presented at the International Meeting on Electrolytic Bubbles organized by the Electrochemical Technology Group of the Society of Chemical Industry, and held at Imperial College, London, 13–14 September 1984.

0021-891X/85 $03.00 + .12

bubble coalescence before they burst on the electrolyte surface appeared to offer considerable potential for reducing emissions.

The methods currently in use include surface active foaming agents, floating plastic spheres and cylinders, local exhaust ventilation and general exhaust ventilation. Foaming agents are expensive and tend to be swept aside by circulation patterns in the electrolyte. Floating spheres and cylinders are effective, but are a nuisance to the operator because they adhere to the cathodes when they are pulled and are relatively expensive. Local exhaust ventilation is effective, but inconvenient and expensive. The large volumes of air required for general ventilation are often used because the method is totally non-interfering. In temperate and cold climates the cost of tempering air can be very high.

2. Background Information

In the numerous studies of the toxicology of sulphuric acid aerosols, their hygroscopicity has not been totally appreciated, as is pointed out by Cavender *et al.* [1]. Also Martonen and Patel [2], who have modelled the dose distribution of sulphuric acid aerosols within the human tracheobronchial tree, suggest that the hygroscopic growth within the human respiratory tract be accounted for when assessing the potential health hazard of airborne particulate matter. Therefore the characterization of the sulphuric acid aerosols should be carried out under controlled relative humidity.

Sulphuric acid aerosols can be classified as *primary* and *secondary*. Mechanical generation of sulphuric acid droplets results in primary aerosols. A mode of this type of generation is the bursting of gas bubbles on the surface of a solution of sulphuric acid such as the zinc electrolyte.

Several investigators in the past have studied the phenomenon of the bursting of single bubbles on a liquid surface as well as that of liquid entrainment. From the bursting of a bubble on a liquid surface two families of droplets are generated: those which come from the bubble dome (film drops) and those which are produced by disintegration of the liquid jet forming in the crater which is left on the liquid surface after the bubble collapses (jet drops) [3].

A critical bubble size has been found, between 4 and 6.5 mm for bubbles in water, beyond which no jet drops are formed [4]. This observation is of importance, since it suggests that control can be effective for the bulk of the emissions ($\geqslant 90\%$) if bubbles are coalesced to the critical size.

The variables on which the critical bubble size depends include density, surface tension, the acceleration due to gravity, and viscosity. It is certain that viscous effects will be second order, and by dimensional analysis it can be shown that critical bubble size is given by the Bond number,

$$\text{constant} = \frac{\sigma}{\rho g d^2_{\text{critical}}} \tag{1}$$

where d_{critical} = the critical bubble size (m), σ = surface tension (N m^{-1} or kg s^{-2}), ρ = density (kg m^{-2}) and g = acceleration due to gravity (approximately $9.81\ \text{m s}^{-2}$). Using this model, the critical bubble size for a commercial zinc electrolyte will be about 90% of that for water without surfactant.

Sizes of film droplets have been reported to be between 0.2 and 10 μm [5] while jet drops are 10–100 times larger at 2–100 μm [3]. The size of jet drops increases as bubble size increases [6–8]. Surface tension does not affect the size of the jet drops from bubbles of the same size, while an increase in viscosity results in smaller droplet sizes [8]. A decrease in surface tension is found to cause a decrease in the number of film drops produced per bubble although the bubble cap area increases for the same bubble size [5].

Three regimes of bubble bursting have been identified in liquid entrainment studies: bursting of single bubbles, bursting of bubbles in a foam layer and destruction of the foam layer and ejection of liquid into the space above the liquid surface. The three regimes follow each other with increasing gas rate [9]. Both families of film and jet drops have been identified in the studies on liquid entrainment [6]. Entrainment increases as gas rate increases in the single bubble bursting regime, reaches a maximum value and then decreases to a minimum due to the formation of a foam layer. Beyond the minimum, entrainment increases slowly with increasing flowrate until destruction occurs, whereupon entrainment

increases drastically. The minimum entrainment has been called *maximum foam protection* and has been attributed to the fact that jet drops are prevented from forming in the case of a foam layer [9, 10]. Decrease in bubble size results in increase in entrainment in the single bubble bursting regime. Entrainment was found to increase in the presence of dispersed substances [11].

Species are transferred selectively from the liquid phase to the air during bubble bursting. Miller *et al.* [12] studied SO_4^{2-} transport by bursting bubbles. He observed SO_4^{2-} enrichment to become more intense in the case of small drops and for high values of surfactant concentration.

The motion of bubbles in an electrolytic cell with gas evolution at the electrode(s), was studied by Wilson [13]. At very low current densities a triangular-shaped wedge is noticed increasing in width from the bottom to the top of the electrode and gas leaves the cell at the electrode–solution interface vicinity. With increasing current density the wedge breaks down and gas bubbles move away from the electrode, circulation of the gas bubbles occurs which extends to higher depths as the gas rate increases. Gas release takes place all over the electrolyte surface.

3. Experimental apparatus and procedures

3.1. *Determination of the electrolyte properties with respect to relative humidity*

Air of a controlled temperature and relative humidity was bubbled through a known volume of the electrolyte and the relative humidity of the air entering and leaving the electrolyte was recorded with time. Equilibrium had been attained for all practical purposes when the air relative humidity at the outlet matched that at the inlet. The acid concentration of the electrolyte at equilibrium was determined chemically and graphically from the plot of the change in the air humidity with time.

Small volumes of electrolyte (5–10 ml) were employed in the process described above in order to shorten the run. This resulted in even smaller volumes of electrolyte after the run and the determination of its density and composition became impossible. Density and composition were determined, then, by using synthetic solutions with the same characteristics as the electrolyte of a series of acid concentrations. In this way the composition of the precipitate which was formed when the acid concentration became higher than a certain value (corresponding to a relative humidity of 60–65% at 20° C) was also determined (by X-ray diffraction).

3.2. *The zinc electrowinning system*

The experimental set-up for zinc electrowinning is shown in Fig. 1. Continuous operation was employed. The neutral and the spent electrolyte were heated to 35° C (mean temperature in industrial cells), mixed at a prescribed ratio and introduced into the cell. The cell was operated at a current density of 615 $A\,m^{-2}$. The voltage drop was approximately 3.5 V. In the cell, zinc was deposited at the cathode at a current efficiency of around 90% and acid was generated. Proper spent electrolyte circulation rate and neutral solution flowrate resulted in steady state operation of the system which corresponded to industrial practice. The electrolytic cell is shown in Fig. 2. It was made of Lucite to facilitate the observation of the bubbles. The interelectrode spacing and the electrode length were close to the ones used in industry. The width was less (~ 10 times) since it was not considered likely that this would affect bubble formation or circulation. Two pairs of working surfaces (anode/cathode) were employed. The electrode material (aluminium for cathode and lead–silver for anode) and the spent electrolyte and neutral solution were provided by Kidd Creek Mines Co.

The composition ($g\,l^{-1}$) of the neutral solution was:

$$Zn : 138.2,\ Mn : 3.9,\ Mg : 6.1$$

and that of the spent electrolyte:

$$Zn : 37.7,\ Mn : 4.1,\ Mg : 5.7,\ H_2SO_4 : 150$$

Impurities were also present in the electrolyte in minor quantities. The density of the electrolyte was 1.23 $g\,ml^{-1}$ and its surface tension 0.07 $N\,m^{-1}$. The frothing agent used in some runs was the Dowfroth 250 (polypropylene glycol methyl ether).

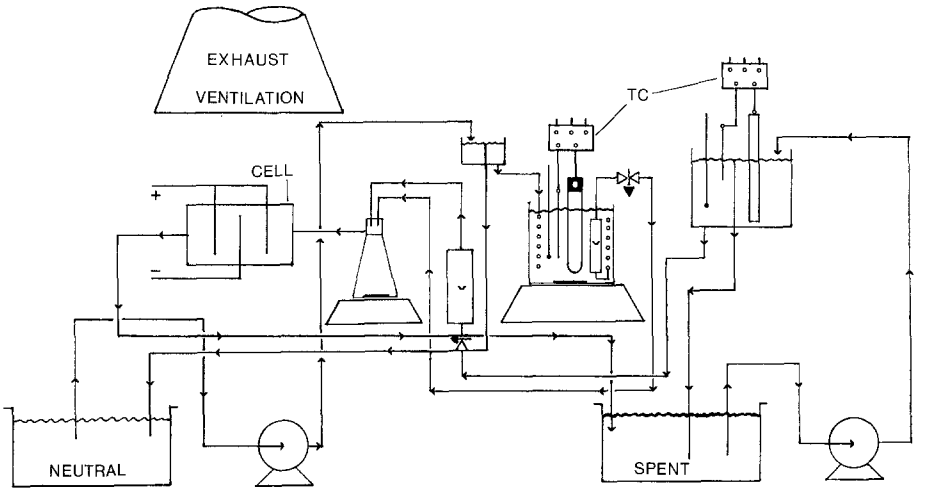

Fig. 1. The zinc electrowinning system.

3.3. *The sampling system*

The aerosol sampling system is shown in Fig. 3. Lucite frames were constructed and fitted above the cell to facilitate the collection of the aerosol at several heights (H) above the cell. The lowest height was 20 cm above the electrolyte surface since this is the distance from the electrolyte surface to the top of the electrodes in practice.

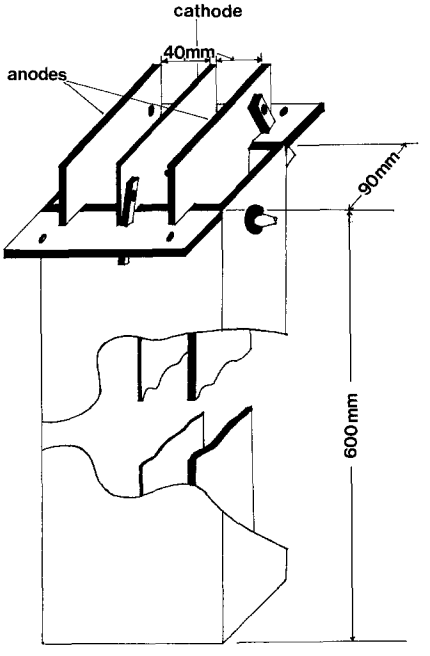

Fig. 2. The electrolytic cell.

The collecting and fractionating device was an inertial impactor (Andersen Samplers Inc.), which was operated upside-down on top of a funnel sitting on the frame. Air was drawn through the impactor by means of a vacuum pump and a flowmeter. At a flowrate of 28.32 $l\,min^{-1}$ the cut-off aerodynamic diameters of the impactor were: 9, 5.8, 4.7, 3.3, 2.1, 1.1, 0.7 and 0.4 μm. After the sample had been collected in the impactor the plates from the stages were placed in Petri dishes and soaked and rinsed with deionized water. The samples were then diluted to 100 ml and analysed for zinc and/or acid and/or sulphate ions.

3.4. *Analytical methods*

The assays of the electrowinning solutions (neutral and spent) were determined by diluting 20 times

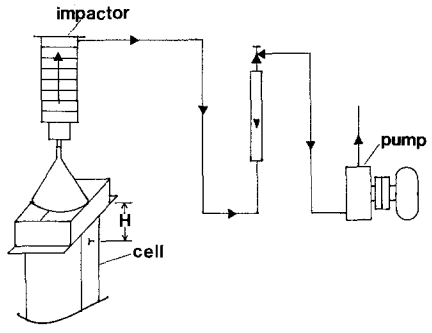

Fig. 3. The sampling system.

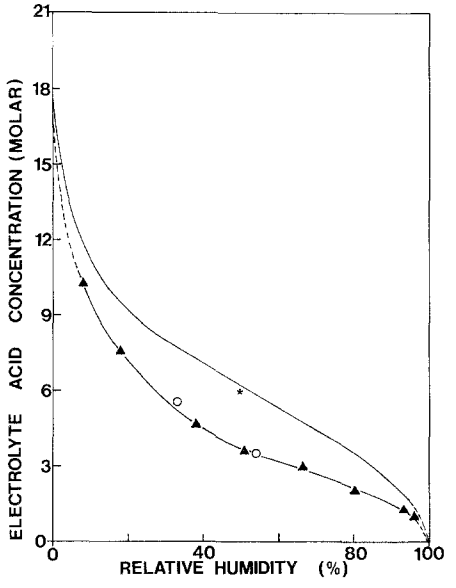

Fig. 4. Sorption isotherm of the zinc electrolyte with respect to relative humidity. Experimental results for: ▲ electrolyte (20° C), * H_2SO_4 (20° C), ○ electrolyte (40° C), —— H_2SO_4 [17].

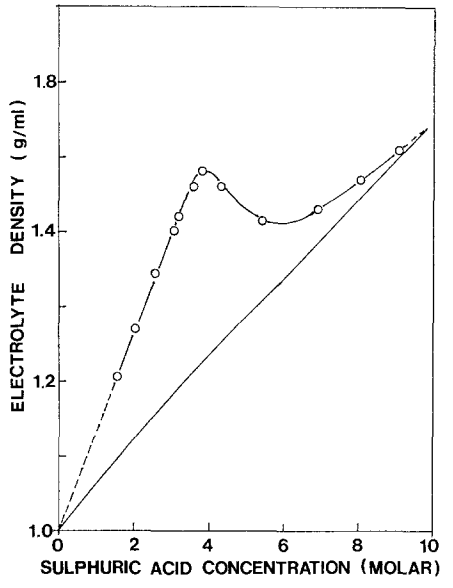

Fig. 5. Electrolyte density as a function of its acid concentration, at 20° C. ○ Electrolyte, —— pure H_2SO_4.

and analysing for acid by titration with standard NaOH, for zinc, manganese and magnesium by complexiметric titration with standard EDTA [14] and for sulphate ions by titration with standard $BaClO_4$ [15].

The aerosol samples after dilution were analysed for acid by titration with standard NaOH (when possible), for zinc by atomic absorption spectrometry and for sulphate ions by either titration with standard $BaClO_4$ for concentrations down to 50 mgl^{-1} or spectrophotometrically using barium chloranilate [16] for concentrations lower than 50 mgl^{-1}.

4. Results and discussion

4.1. *Relative humidity effect on the aerosol characteristics*

Fig. 4 shows the electrolyte sorption isotherm with respect to the air relative humidity at 20° C. In the same figure the sorption isotherm for pure H_2SO_4 is plotted from values given in CRC Handbook of Chemistry and Physics [17]. The difference between the isotherms for electrolyte and pure H_2SO_4 is due to the presence of dissolved salts in the electrolyte. The points which correspond to 40° C temperature indicate that the isotherm at 40° C does not differ significantly from that at 20° C.

Fig. 5 illustrates the variation of the electrolyte density with the acid concentration. The curve approaches asymptotically that of the pure H_2SO_4 at high acid concentrations. Precipitate appeared at acid concentrations higher

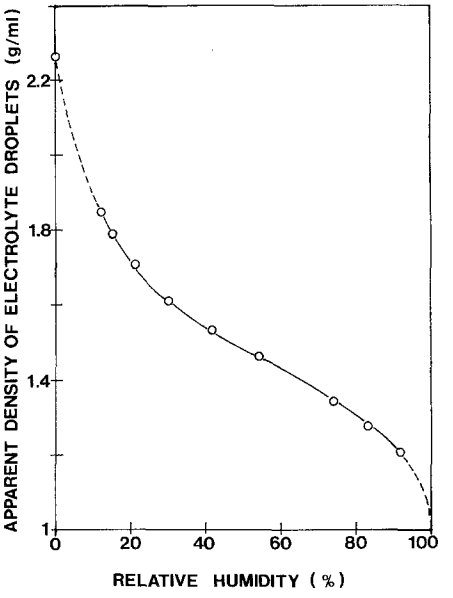

Fig. 6. Apparent density of electrolyte droplets as a function of air relative humidity.

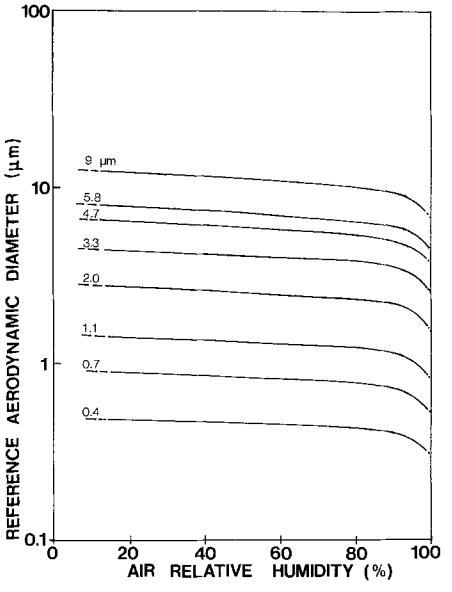

Fig. 7. Reference aerodynamic diameter of aerosol droplets of various aerodynamic diameters as a function of relative humidity.

than 3.2 M. It was found to consist of $ZnSO_4 \cdot H_2O$, $MnSO_4 \cdot H_2O$ and $MgSO_4 \cdot H_2O$. Due to this precipitation, the density of the aerosol droplets is not that shown in Fig. 5. Instead, an apparent density can be calculated if the volume and mass of the precipitate are incorporated and the results are presented in Fig. 6.

Aerosol size distributions must be corrected to a reference relative humidity, since equilibrium sizes depend on relative humidity. The equilibrium relative humidity (90%) of the electrolyte as it is used in the cell was chosen as the reference. Fig. 7 provides the aerodynamic diameter a droplet would have at 90% r.h. if its diameter were determined at a humidity other than 90%. Results have been derived with the help of Figs. 4 and 6 and are shown for the cut-off sizes of the impactor.

4.2. *Generation, motion and bursting of bubbles in the electrowinning cell*

The acidic aerosol emitted from zinc electrowinning cells is the product of the bursting of bubbles of hydrogen and oxygen during the electrowinning process. The size of the gas bubbles is determined by parameters such as surface tension and viscosity of the electrolyte and structure of the surface of the electrodes, factors which depend on temperature and quality of the electrolyte. Of the above three parameters only the last one undergoes significant variation during the electrowinning process because of the side reactions occurring at the anode. The main side reaction occurring at the anode, in addition to oxygen evolution, is oxidation of Mn^{2+} to form MnO_4^- and MnO_2. MnO_4^- diffuses into the bulk of the electrolyte while most of the MnO_2 deposits as a scale on the anode and grows thicker with time. This scale provides a smoother surface with large scale features which promotes the generation of larger bubbles as compared to the electrode without the scale. In industrial practice the MnO_2 scale is removed (descaling) every 20–40 days. Descaling of the anode results in the generation of smaller bubbles. The bubbles become larger, as the scale grows, and attain a steady-state after approximately 40 h of operation. Sizes of bubbles were found to increase more than 50% because of the scale formation, as shown in Fig. 8.

The bubbles after their detachment from the electrodes move upwards. Since the rate of generation of gases is almost uniform along the electrodes, the gas hold-up increases from the bottom to the top of the electrode. A gross mean hold-up of approximately 2.5% was measured. The motion

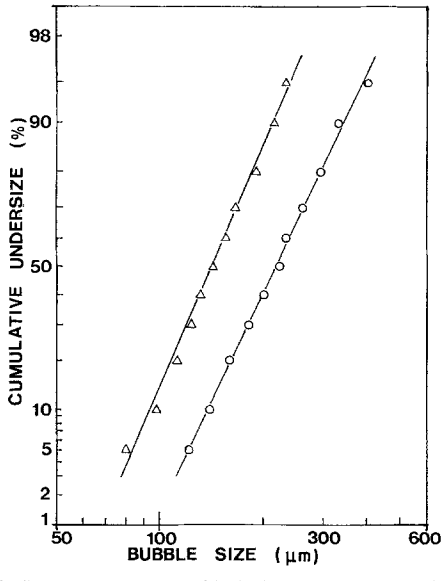

Fig. 8. Size distributions of bubbles in the electrowinning cell, showing effect of MnO_2 scale. △ Descaled and ○ stabilized anodes.

of bubbles occurs in a wedge-type formation at the bottom of the electrodes which, however, breaks down higher in the cell where motion of bubbles towards the centre of the interelectrode spacing is observed and circulating streams of bubbles are established. Coalescence of bubbles occurs during their motion in the electrowinning cell. The rate of coalescence is proportional to the bubble density in the electrolyte and is expected to be higher the smaller the bubbles are and/or the closer the bubbles are to the electrolyte surface, since circulation of bubbles is observed there. The rate of coalescence is inhibited by the presence of dispersed MnO_2 in the electrolyte, presumably because of its hydrophylic behaviour. MnO_2 forms in the bulk of the electrolyte from the reaction of MnO_4^- with Mn^{2+} which is particularly favoured after the anodes have been descaled. This is one more reason for the smaller sizes of bubbles associated with the descaled anodes.

During the wedge-type formation of the motion of bubbles, larger bubbles occupy the inner part of the wedge and smaller ones the outer. The circulation streams found higher in the cell consist mainly of smaller bubbles, which undergo coalescence and finally burst on the electrolyte surface. Discharge of bubbles occurs more easily at the electrode–electrolyte–air boundary where surface tension forces are lower; however, bubbles burst as assemblages of bubbles or as single bubbles all over the electrolyte surface. Increase in the number of bubbles (gas flowrate), decrease in the size of bubbles or increase in floating time of bubble before bursting (i.e. decrease in surface tension) result in full coverage of the surface with bubbles and, eventually, foam formation.

The bursting of bubbles on the electrolyte surface results in the formation of droplets, as products of the disintegration of both the liquid film of the bubble dome (film drops) and the liquid jet forming in the crater left in the liquid after the rupture of the bubble dome (jet drops). Jet drops are larger in size and are ejected vertically while film drops are smaller and are ejected at any angle from 0 to 180°. When assemblages of bubbles are present jet drops may also be ejected at an angle from the vertical because of the bursting of a smaller bubble inside the cavity of a larger nearby bubble which burst earlier. Bubbles bursting in a foam layer do not produce jet drops at all, since the foam layer acts as a shock absorber for the waves which proceed down the bubble crater and result in the formation of the liquid jet. Jet drops also do not form from bubbles of sizes above a critical size which is in the range of 4–6.5 mm and decreases with decreasing surface tension and increasing density of the liquid phase. The critical size is the size for which the submerged portion of the floating bubble is almost a hemisphere. Below this size the protruding portion is smaller than the submerged one and above it the submerged portion is smaller and significantly distorted from the spherical shape. The liquid 'rushes' to fill the submerged portion of the concentrates at the centre of curvature. The centre of curvature is below the still liquid surface (state of lowest potential) for small bubble sizes. Larger sizes have more than one centre of curvature (because of distortion) located above the still surface and the result is insufficient energy for the formation of jet droplets. Under normal conditions of operation, the bubbles in the electrowinning cell are far smaller than the critical size (100–500 μm) (Fig. 8).

The size of jet drops increases and the number of jet drops produced per bubble decreases as bubble size increases. This observation is in satisfactory agreement with the jet formation mechanism discussed in the previous paragraph. Experimental findings in the literature provide relations between the number of film drops and area of bubble dome, and area of bubble dome and bubble size. For constant gas flow rate calculations show that the number of film droplets produced increases as the size of bubbles decreases.

4.3. *Characterization of the acidic aerosol*

Table 1 shows the amounts of H_2SO_4 and Zn collected by the impactor on its stages and their ratios. The ratio is shown to be independent of size and is equal to the ratio of the two species in the electrolyte. The size distribution is plotted in Fig. 9. The change in slope indicates a bimodal distribution. 90% of the mass of the aerosol is above 10 μm. The top part of the distribution represents the jet drops and the bottom the film drops. Because of the small percentage of the mass that the film drops represent, the distribution

Table 1. Amounts of H_2SO_4 and Zn collected on the stages of the impactor and their ratios

Impactor stage	*H_2SO_4 (mg)*	*Zn (mg)*	*Zn (mg)/H_2SO_4 (mg)*
Preseparator + 0	113.4	29.2	0.26
1	9.7	2.4	0.25
2	1.7	0.42	0.25
3	2.5	0.66	0.26
4	0.34	0.092	0.27
5	0.20	0.054	0.27
6	0.098	0.024	0.24
7	0.049	0.016	0.33
Filter	–	0.008	–

of the jet drops can be considered not to be affected by them. The geometric standard deviation σ_g of the top part of the distribution is found to be 2.4. The σ_g of the distribution of the film drops is 1.4.

Table 2 shows the amounts of Zn^{2+} and SO_4^{2-} and their ratios at the several stages of the impactor. It appears that ratios become smaller as sizes become smaller which indicates SO_4^{2-} enrichment in small droplets. The ratios at the top stages are quite close to the ratio of the two species in the electrolyte.

Entrainment rates (total mg H_2SO_4 min^{-1}) at the reference height of 20 cm above the electrolyte surface varies from 0.50 to 1.30 mg H_2SO_4 min^{-1} (2–3 mg m^{-2} s^{-1}). However, in runs which were performed right after descaling of the anodes values varied between 0.84 and 1.55 mg H_2SO_4 min^{-1}. Moreover the use of a frothing agent (Dowfroth) resulted in a reduction in emission rates to 0.47 and 0.46 mg H_2SO_4 min^{-1}. The size distributions obtained in these two cases are also plotted in Fig. 9. After descaling smaller bubbles were generated in the cell which resulted in smaller and more numerous jet drops as Fig. 9 shows. The bubbles are small when the frothing agent was used as well. However, other characteristics of the bubbles also change, such as surface activity, stability of bubble (thickness of bubble dome during rupture) etc. It appears from Fig. 9 that film drops form a larger percentage of the total aerosol mass in the presence of a frothing agent.

4.4. *Control of the acidic aerosol resulting from zinc electrowinning cells*

The acidic aerosol generated from the electrowinning cells is a direct function of the characteristics of the bubbles in the cell. Therefore emissions (amounts and characteristics) are altered when the characteristics of the bubbles are altered. A new method of control has been developed which reduces the emissions by providing means of bubble coalescence before their bursting on the electrolyte surface. One conception of the

Table 2. Amounts of Zn and SO_4^{2-} collected on the stages of the impactor and their ratios

Impactor stage	*Zn (×10 mg)*	*SO_4^{2-} (×10 mg)*	*Zn (mg)/SO_4^{2-} (mg)*
Preseparator + 0	19.65	119.0	0.16
1	0.98	6.5	0.15
2	0.20	1.38	0.14
3	0.34	2.55	0.13
4	0.034	0.63	0.054
5	0.031	0.49	0.063
6	0.027	0.63	0.043
7	0.015	0.65	0.023
Filter	0.008	–	–

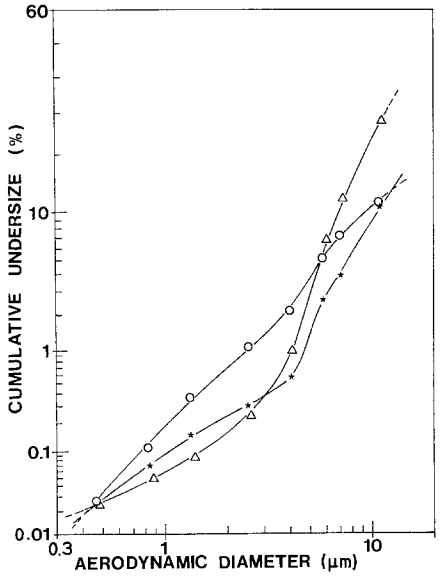

Fig. 9. Aerosol size distribution. * Stabilized anodes, ○ use of frothing agent, △ descaled anodes.

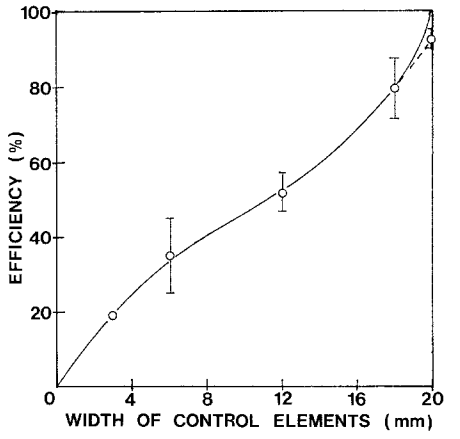

Fig. 11. Efficiency (%) of control elements versus their width.

method requires the use of a pair of elements placed on the electrodes (Fig. 10) and immersed in the electrolyte. The elements merely act as a mechanical structure to bring the bubbles in close contact and thus promote interbubble coalescence. Bubbles are intercepted at the surface of the elements on their way to the electrolyte surface. Coalescence of the bubbles arriving at and on the surface occurs. Thus, bubbles grow on the surface of the elements and are larger when bursting on the electrolyte surface. Drainage of the liquid film separating the bubble from the solid surface occurs and when it ruptures viscous forces become negligible. After the rupture of the liquid film, the bubbles move under the effect of drag forces from the moving electrolyte. Thus, the retention time of the growing bubbles on the solid surface, and therefore, the degree of coalescence, is determined by the drainage time of the liquid film. This last quantity depends on the properties of the liquid and the size of the bubble.

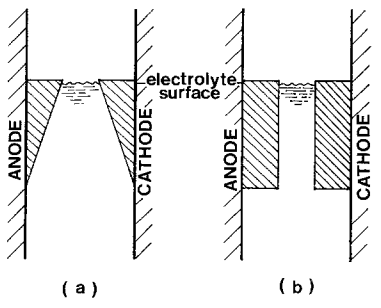

Fig. 10. Control elements (a) triangular-shaped, (b) square-shaped.

Tests were performed with both triangular and square-shaped control elements (Figs. 10a and b) and their efficiencies were not significantly different. Efficiency was also found to be independent of the depth of the elements. A relationship, however, was established between the width of the control elements and their efficiency, which is shown in Fig. 11. The change in the curvature of the curve indicates the change in the mechanism of control associated with the use of the large control elements. In the latter case, on the one hand bubbles may have exceeded the upper limit for the production of jet drops and on the other the foaming power of the system is enhanced due to the smaller area of exposed liquid surface.

Size distributions of the aerosol from the control elements are shown in Fig. 12. The size distributions of the aerosol emitted in the presence of all but one of the control elements showed no significant difference from those obtained without the elements. The run associated with the highest efficiency obtained using the largest element gave aerosol distributions which were shifted towards smaller sizes which may be the result of the absence of jet drops from bubbles above the critical size and/or foam formation.

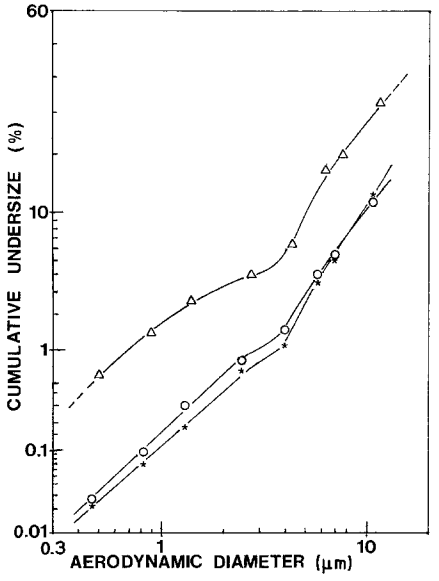

Fig. 12. Aerosol size distributions in the presence of control elements. * Without control elements, ○ 12 mm and △ 18 mm control elements.

5. Conclusions

The following conclusions can be drawn from the work reported here:

(a) Air relative humidity affects the aerodynamic size of the acidic aerosol resulting from zinc electrowinning cells.

(b) Two families of drops are generated by the bursting of gas bubbles on the zinc electrolyte surface: jet and film drops. Film drops form only a small percentage of the total aerosol mass.

(c) Control of mist emissions can be achieved by coalescing gas bubbles below the electrolyte surface. Extensive research describing means of achieving this will be submitted for publication shortly.

Acknowledgement

The authors gratefully acknowledge financial assistance from the Ministry of Labour. Kidd Creek Mines Co. kindly supplied the materials used in the present study. Discussions with our colleagues, and especially R. L. Hummel and D. H. Napier were most productive.

References

[1] R. L. Cavender, J. L. Williams, W. H. Steinhagen and D. Woods, *J. Toxicol. Environ. Health*, 2 (1977) 1147.
[2] T. B. Martonen and M. Patel, *J. Amer. Ind. Hyg. Assoc.* **42**(6) (1981) 453.
[3] F. MacIntyre, *J. Geophys. Res.* 77(27) (1972) 5211.
[4] Y. Toba, *J. Oceanogr. Soc. Jpn.* **15**(3) (1959) 1.
[5] M. P. Paterson and K. T. Spillane, *Quart J. R. Met. Soc.* **95** (1969) 526.
[6] F. H. Garner, S. R. M. Ellis and J. A. Lacey, *Trans. Instn. Chem. Eng.* **32** (1954) 222.
[7] D. C. Blanchard, 'The Electrification of the Atmosphere by Particles from Bubbles in the Sea', in 'Progress in Oceanography', Vol. 1, MacMillan, New York, (1963) p. 71.
[8] N. Mitsuishi, S. Sakata, Y. Matsuda, Y. Yamamoto and Y. Oyama, 'Studies on Liquid Entrainment', AEC-tr-4225, 1961 (Translation of three Japanese papers).
[9] V. G. Gleim, *J. Appl. Chem. USSR* **28**(1) (1955) 9.
[10] V. G. Gleim, *ibid.* **26**(11) (1953) 1099.
[11] E. M. Lavrova, *ibid.* **46**(8) (1973) 1848.
[12] C. W. Miller, W. V. Kessler and V. L. Anderson, *Environ. Lett.* **10**(1) (1975) 1.
[13] C. J. Wilson, MSc Thesis, University of Manchester (1970).
[14] A. Vogel, 'Vogel's Textbook of Quantitative Inorganic Analysis', 4th ed., Longman, New York (1978) p. 330.
[15] Niosh, 'Manual of Analytical Methods', Vol. 3, 2nd ed., US Department of Health, Education, and Welfare, Cincinnati (1977).
[16] H. N. S. Schafer, *Anal. Chem.* **39**(14) (1967) 1719.
[17] 'CRC Handbook of Chemistry and Physics', 59th ed., (edited by R. C. Weast and M. J. Astle) CRC Press (1978).